Review article

Dieter Bimberg*

Semiconductor nanostructures for flying q-bits and green photonics

https://doi.org/10.1515/nanoph-2018-0021
Received February 19, 2018; revised April 26, 2018; accepted April 27, 2018

Abstract: Breakthroughs in nanomaterials and nanoscience enable the development of novel photonic devices and systems ranging from the automotive sector, quantum cryptography to metropolitan area and access networks. Geometrical architecture presents a design parameter of device properties. Self-organization at surfaces in strained heterostructures drives the formation of quantum dots (QDs). Embedding QDs in photonic and electronic devices enables novel functionalities, advanced energy efficient communication, cyber security, or lighting systems. The recombination of excitons shows twofold degeneracy and Lorentzian broadening. The superposition of millions of excitonic recombinations from QDs in real devices leads to a Gaussian envelope. The material gain of QDs in lasers is orders of magnitude larger than that of bulk material and decoupled from the index of refraction, controlled by the properties of the carrier reservoir, thus enabling independent gain and index modulation. The threshold current density of QD lasers is lowest of all injection lasers, is less sensitive to defect generation, and does not depend on temperature below 80°C. QD lasers are hardly sensitive to back reflections and exhibit no filamentation. The recombination from single QDs inserted in light emitting diodes with current confining oxide apertures shows polarized single photons. Emission of ps pulses and date rates of 10^{10} + bit upon direct modulation benefits from gain recovery within femtoseconds. Repetition rates of several 100 GHz were demonstrated upon mode-locking. Passively mode-locked QD lasers generate hat-like frequency combs, enabling Terabit data transmission. QD-based semiconductor optical amplifiers enable multi-wavelength amplification and switching and support multiple modulation formats.

Keywords: quantum dot growth and electronic properties; quantum dot lasers; ultra-fast lasers and amplifiers; single q-bit emitters.

1 Introduction

The discovery, development, and use of novel materials and technologies were decisive for the development of civilizations across the last ten thousand years. The silicon age, as many call the 20th century, enabled storage and processing of data and information. This age started with the discovery and use of silicon – a rather new material – when measuring time in segments of thousands of years. The "light age", as many are calling the 21st century, is characterized by the advent of novel illumination, communication, and alternative energy technologies based to a large extent on compound semiconductor devices, efficiently emitting, modulating, amplifying, or absorbing photons. These devices and again Si-based ones present a basis for a sustainable society. An increasing number of the basic materials are nanostructures, like lasers based on quantum wells. They are omnipresent in so many consumer and communication systems, but without these, most users are realizing the importance of the nanostructures for functionality.

In the past, "new" materials were based on chemical engineering of novel compounds. Chemical composition changes of known materials and doping or the inclusion of known but rare materials change their properties. With the advent of nanomaterials, nanotechnologies, and nanodevices, we discover that size and shape are more than just another subject of researchers' curiosity in ultra-small objects. Nanotechnologies enable us to modify the properties of materials, complex structures, and devices based upon them without changing their composition.

The ultimate class of such nanostructures, "quantum dots" (QDs), have lateral dimensions in all three directions that are smaller than the de Broglie wavelength

***Corresponding author: Dieter Bimberg,** Institute for Solid State Physics, Technical University Berlin, Berlin, Germany, Phone: +491702454615, Fax: +493031422569, e-mail: bimberg@physik.tu-berlin.de. http://orcid.org/0000-0003-0364-6897; and Chinese-German Center for Green Photonics of the Chinese Academy of Sciences, CIOMP, Changchun, China

of the charge carriers. They constitute nanometer-size coherent clusters that are embedded in the dielectric matrix of another material [1–6]. The term "QD" appeared in open literature for the first time in 1986, when two papers were published (see web of science). Until 1989, a total of 43 publications referred to QDs. Between 1990 and 1999, the number of publications exploded to 6211. Today, in March 2018, more than 110,000 publications and books dealing with QDs have appeared. It is thus impossible to give justice in this short, non-exhaustive review to at least the authors of the most important contributions, which recently appeared in this vigorously developing field, and refer to their work or to cover all of the rapidly emerging subjects, like nanoflash memories, VECSELs, or SESAMs.

In semiconductor epitaxy, the growth of QDs is now well understood [7–12]. They are often observed being self-similar and can be formed by self-organized growth on surfaces [9–11]. Single QDs enable novel devices for quantum cryptography, quantum information processing, and novel dynamic random access memories (DRAM)/flash memory cells [13–16]. Billions of them present the active areas in optoelectronic devices like ultra-large bit rate and energy-efficient QD lasers or QD optical amplifiers, potentially revolutionizing communication, consumer electronics, or measurement systems [17–19].

We will focus here on some of the first important achievements. The essential physics laws driving the self-organized growth of QDs are summarized. Then we focus on their absolutely unique electronic and optical properties before we resort to some of the most important photonic devices based on single or millions of QDs.

2 The prehistoric times of nanomaterials and photonics

The advent of semiconductor nanomaterial-based photonics can be dated back to 1976, when Ray Dingle and Chuck Henry from Bell Labs received a US patent entitled "Quantum effects in heterostructure lasers" [20]. The essential argument of the patent was, a "reduction of dimensionality", going from "three-dimensional" (3D) (bulk) materials in double heterostructure lasers; to two-dimensional (2D) materials, quantum wells; and eventually to one-dimensional (1D) materials, quantum wires, is leading step by step to orders of magnitude reduction of the threshold current density of the lasers. Today, 42 years later, most of the semiconductor lasers are indeed quantum well lasers. Their fabrication by metal organic chemical vapor phase deposition (MOCVD) or molecular beam epitaxy (MBE) is easy; the gain layer(s) has a thickness in the nanometer range (below the de Broglie wavelength). Strange enough, Dingle and Henry did not discuss potential advantages of zero-dimensional structures in their patent application.

It took another 10 years, or until 1986 [21], for a group of researchers led by Suematsu at the Tokyo Institute of Technology to present a detailed theoretical comparison of gain and threshold current density for GaAs and InP-based zero-dimensional (quantum box) to 3D lasers, predicting enormous improvements for zero-dimensional "quantum box" lasers, like a strong reduction of the threshold current density. Earlier, in 1982, Arakawa and Sakaki [22] had experimentally investigated GaAs-based QW lasers in high magnetic fields and observed a reduction of temperature dependence of threshold current with increasing magnetic field and attributed this observation to the increased carrier localization. All these works [20–22] in the seventies and eighties were based on considering solely lattice matched structures. Lattice match was considered to be imperative for semiconductor heterostructures at that time to avoid formation of defects, like dislocations. Many groups in the world embarked then on trying to fabricate such lattice matched quantum box/dot lasers, mostly by combining lithography with epitaxy. Seven years later, such laser [23] based on the

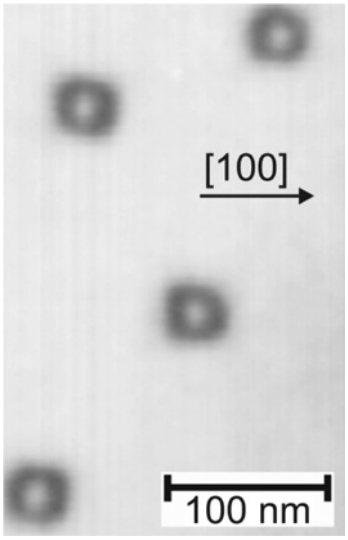

Figure 1: High-resolution top-view transmission electron microscopy picture of a layer of InAs/GaAs QDs, showing four pyramidal dots.
The basis of the pyramids is oriented parallel to [100] directions of the semiconductor, from Refs. [10, 11].

best available InP technology was presented by the Tokyo Institute of Technology group, showing a threshold current density of 7.5 kA/cm^2, much larger than predicted in Ref. [21], operating in a pulsed mode at 77 K. These and other similar results were regarded as discouraging.

A new dawn appeared in 1993/4, when self-organization at semiconductor surfaces upon deposition of a few monolayers of non-lattice matched InGaAs on top of GaAs was discovered to lead to the formation of coherent (meaning defect-free) self-similar nanometer-sized pyramids, QDs [1–6], see Figure 1. These QDs exhibited close to delta function-like cathodoluminescence spectra [24] (as was later discovered: Lorentzian shaped). Lasers with such QDs as gain material were rapidly discovered to show operation at the low threshold current densities hoped for [25].

3 The key to strain-driven self-organized growth

Volume elastic relaxation of coherently strained islands has been discovered and described in detail theoretically in the nineties as an alternative mechanism of total energy relaxation competing with the formation of dislocations [7, 8, 12]. The total energy E_{total} of a heterostructure lattice-mismatched system with islands having edges is equal to three contributions: the relaxation of elastic energies, the variations of the surface energies, and the discontinuity of the intrinsic surface stress tensor at the edges. $E_{total} = E_{elastic} + E_{surf} + E_{edges}$. Cubic semiconductors are elastically anisotropic. Their surface energies depend on the type of surface reconstruction, which in turn depends on temperature, crystallographic orientation, and strain. For any given amount of strained material deposited at any temperature and any surface orientation, there exists an equilibrium size and shape. Detailed calculations reveal pyramidal shapes of QDs with axes elongated along the [100] directions of the semiconductor for (100) substrates to provide maximum energy relaxation in thermodynamic equilibrium [7, 8]. The formation of QDs is thus driven by self-organization (called often Stranski-Krastanow process) and leads to self-similarity of the QDs (see Figure 1). Spontaneous formation of spatial, temporal, or spatio-temporal patterns by self-organization of individual constituents is a common phenomenon in nature, as pointed out by Haken [7, 8] and others more than 30 years ago.

In consequence, the fabrication of self-organized QDs, similar to that of QWs, is based on a non-disruptive growth technology, which works for any strained material system (e.g. also for InN/GaN). Complex and costly electron beam lithography is thus unnecessary. Self-organized QD growth relies simply on modifications of the parameters of classical semiconductor epitaxial processes (let it be MBE or MOCVD) and uses a before undiscovered parameter window for the growth of defect-free strained layers. Brilliant high-resolution transmission electron micrographs of InAs/GaAs QDs (Figure 1) that were grown using MOCVD [10, 11] reveal indeed a close to perfect self-similarity of QDs and confirm the thermodynamic modelling approach [7, 8]. Further important theoretical work included kinetic aspects [12] and contributed to a more detailed understanding of QD growth.

4 Electronic and optical properties of atoms in a dielectric cage: the QD case

Shape and composition of QDs are the essential input parameters, needed for any quantitative modelling of electronic properties. They can be revealed by combining plane view and cross-section transmission electron microscopy [9] or scanning tunneling microscopy [26]. Once the material distribution inside and outside a QD is known, one can calculate the strain field by e.g. continuum theory [1–8]. Knowledge of the strain field allows the determination of the piezoelectric potentials. The most advanced and, at the same time, lucid calculation of the electronic structure of QDs uses a numerical 8-band strained k.p model including piezoelectric effects [27]. Figure 2 gives the delta-function energy levels and wave functions of a 45° pyramidal InAs/GaAs QD of 13.3-nm base length obtained by a 8-band k.p model.

The most important feature of the electronic structure is that In QDs do not exist in “free carrier” states with momentum-dependent dispersion of the energy but only in fixed-energy states like in atoms. Energy sublevel positions and thus the wavelengths of recombination are strongly dependent on the geometry of the QDs. A beautiful demonstration of the tunability of the emission of (InGa)As/GaAs QDs by varying the geometry and the composition is given in Figure 3.

The experimentally measured peak energies in these MOCVD grown structures range from about 1050 nm to more than 1400 nm. Emission beyond 1600 nm was demonstrated for growth on metamorphic buffers by MBE [28]. Deposition of the QDs within a large-bandgap AlGaAs matrix results in a shift of the emission wavelength towards

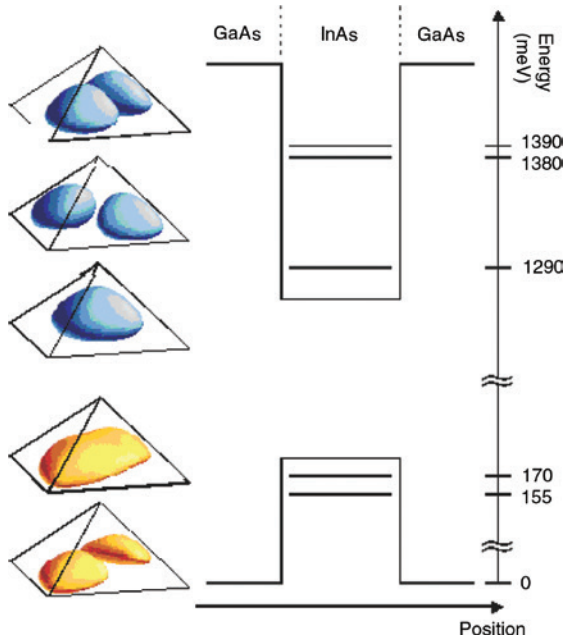

Figure 2: Wave functions and energy levels for the three lowest electron and two lowest hole eigenstates in a pyramidal InAs/GaAs QD.
The calculation was done using 8-band k.p-theory, from Refs. [1–3].

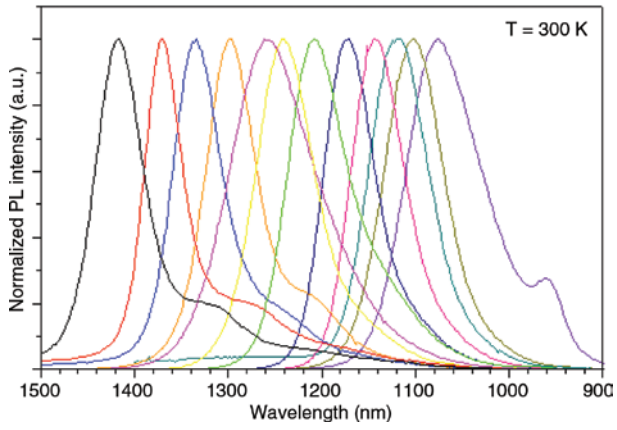

Figure 3: The wavelength of emission from the excitonic ground state of a QD can be varied by varying its size and composition and that of the matrix.
The figure shows the variation of the normalized PL spectra of various InGaAs ensembles in an AlGaAs matrix, taken from Refs. [1–3].

the visible range. Thus, GaAs-based QD technology allows for an emission or absorption wavelength tuning between the red and the infrared. In particular, the "spectral hole" between 1100 nm and 1270 nm where high-performance lasing was hard to obtain before for standard GaAs- and InP-based technologies is now filled. Figure 4 summarizes the impact of changes of dimensionality on the electronic density of states in a semiconductor (schematically).

In a 3D (volume) direct gap semiconductor, the wave vector **k** is a good quantum number and the ideal density of states is proportional to the square root of the energy. A continuous density of state results in a broad, temperature-dependent distribution for a given number of charge carriers. For quantum wells (2D) and quantum wires (1D), the components of the wave vector in the direction of quantization are no good quantum numbers any more. Yet, the density of states is still continuous and carriers obey a thermal occupation. Inhomogeneous broadening induced e.g. by realistic interface fluctuations leads to smearing out of the ideal density of states. Only QDs show a complete quantization, resulting in discrete energy levels and no inhomogeneous broadening or Maxwellian tails of the luminescence upon level occupation by charge carriers at finite temperatures.

It is of decisive importance for applications in quantum communication or spintronic [13–15] that in a QD of zinc-blende structure, the energy levels are spin-degenerate only. Figure 2 shows a QD of pyramidal shape whose structure in the base plane has C_{4V} symmetry. Due to the strain-induced piezoelectric potentials, the symmetry of the confining potential is, however, lowered to C_{2V}. A splitting of the excited $p_{x,y}$-states to two spin-doublets results [27]. The centers of charge of electron and hole wave functions are not identical but depend on the actual distribution of atoms inside the QD. For an example of a homogeneous distribution of In atoms in the QD used in Figure 2, the electron wave function is located on top of the hole wave function, creating a dipole moment. An increased concentration of In atoms at the top of a ternary InGaAs QD [29, 30] can, however, result in the opposite ordering of wave functions and an inversion of the dipole [29–31].

The 8-band k.p approach also allows calculations of wavefunctions in sheets of vertically coupled QDs – in analogy to super-lattices. The device-relevant ratio of TE to TM polarization can be tuned by a variation of spacer thickness [29–31]. Eight-band k.p theory single-particle wave functions present the input to calculate the energy states in QDs containing more than one charge carrier, let it be electrons or holes, when Coulomb interaction becomes essential.

Coulomb interaction, anisotropic exchange, and correlation have a large impact on many particle states, like excitons, trions, and biexcitons, due to the strong localization of the charge carriers. The actual contribution of each term depends strongly on the shape, size, and material composition of the dot. The electron-hole exchange interaction lifts the fourfold degeneracy of the excitonic ground state into two optically active and two inactive states. The lowering of the confinement symmetry

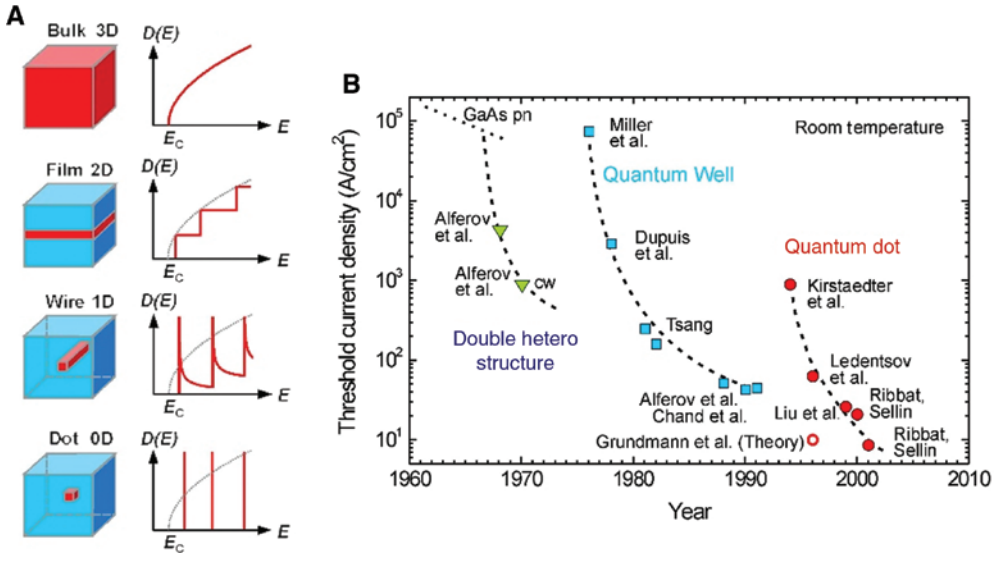

Figure 4: Effect of reduced dimensionality.
(A) Charge carriers are confined in a semiconductor (red) with a smaller bandgap than the cladding semiconductor (blue). The confinement changes the density of states D(E). E_c is the conduction-band edge of a 3D semiconductor, from Ref. [4]. (B) Development of the threshold current density of semiconductor lasers between their invention and the rord values for QD-lasers.

by piezoelectric potentials (see above) results in turn in a fine-structure splitting E_{FS} of the exciton ground state. A doublet structure of the exciton and biexciton recombination results [29–31], see Figure 5.

The fine-structure splitting E_{FS} as well as the biexciton binding energy (the energy difference between biexcitonic and single excitonic recombination) depends on the size of the QD. For both values, a monotonous decrease with QD size has been observed. A transition from positive to negative fine-structure splitting and biexciton binding energy occur [29–31]. This observation is beyond our experience from classical atomic physics, where no "anti-binding" H_2 molecule exists. Both values can be also zero for a QD of the right size and shape, which is of importance for applications of single QDs as q-bit and entangled photon emitters.

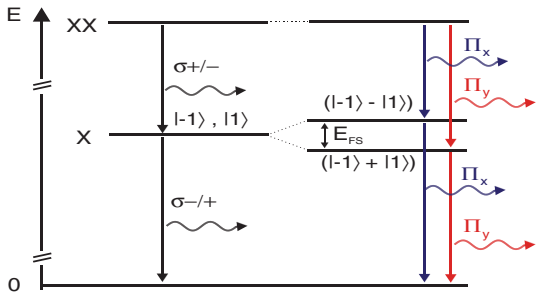

Figure 5: Excitonic and biexcitonic recombination of an InAs/GaAs QD without piezoelectric (left) and with piezoelectric effects, which lower the symmetry from C_{4v} to C_{2v}. E_{FS} is the fine structure splitting. The polarizations of the transitions are shown.

5 Single QDs as q-bit or entangled photon emitters

Our daily life depends more and more on secure data communication. Combining basic principles of quantum mechanics with most modern information theory allows the introduction of quantum communication schemes, like those first proposed by Bennett and Brassard (BB84 protocol) [13–15]. The "Quantum Information Science and Technology Road Map", developed on behalf of the Advanced Research and Development agency (ARDA) of the US government, asks for the development of inexpensive practical sources of single photons of well-defined polarization, called q-bits, for the realization of the BB84 and more advanced protocols and/or for sources of entangled photon pairs.

A single semiconductor QD with its discrete delta-function-like excitonic ground state, allowing for non-resonant excitation, has decisive advantages as compared to any other system e.g. isolated atoms [13–15]. Being embedded in a suitable p-i-n structure, an electrically driven high frequency pulsed source of single photons, q-bits on demand, can be realized.

A module operating at 300 K, based on such devices, would not cost much more than a "normal" semiconductor LED for data communication.

Controlled growth of epitaxial layers with extremely low densities of QDs of 10 [13–15] cm^2 has indeed been realized on top of oxide apertures localizing single QDs

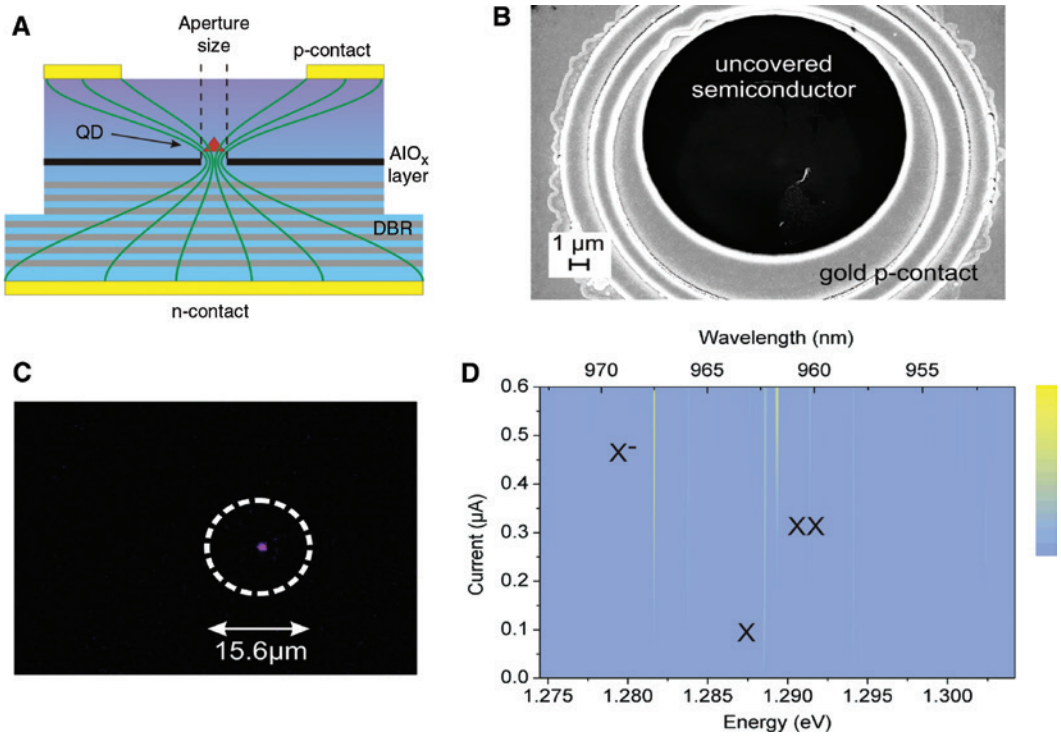

Figure 6: (A) Schematic cross-section of a single electrically driven q-bit emitter with one Bragg reflector showing the QD position, aperture size, and current flow, from Refs. [32–34]. (B) Scanning microscopy image of an electrically driven SPE. (C) Single q-bit emission from a single QD. (D) Spectra of a single exciton, a trion, and an excitonic molecule from the device shown in B as a function of current. With increasing current the single exciton emission saturates, from Refs. [32–34].

in InAs/GaAs structures. Such layers were embedded in p-i-n diode structures with a distributed Bragg reflector (DBR) and complete resonant micro-cavities to enhance the emission rate via the Purcell effect to have directed emission and a large output yield. Figure 6A shows a schematic cross-section of a single photon emitter (SPE) with one DBR.

The spectrum in Figure 7 shows the emission of a different electrically driven SPE across a spectral region of more than 400 nm. Only one (polarized doublet) emission line, caused by the fine-structure splitting of the exciton ground state, is observed at 950 nm.

These devices were driven at repetition rates of 1 GHz using electrical pulses of 350-ps width. Figure 8 shows traces of an auto-correlation experiment obtained from a trion (charged exciton) emission. The second-order auto-correlation function value $g^{(2)}(0) = 0.05$ proves to be an almost ideal antibunching of the single polarized photons, the q-bits [13–15].

Creation of entangled photon pairs is a precondition for quantum repeaters, enabling quantum communication across longer distances. A promising proposal for the creation of entangled photon pairs relies on the biexciton- to exciton- to ground-state recombination

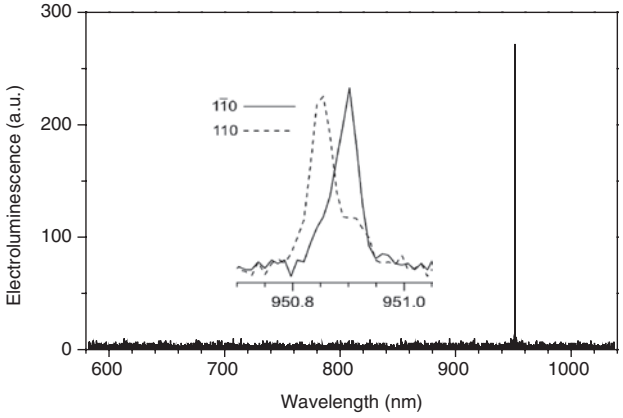

Figure 7: Emission of an electrically driven q-bit (single photon emitter).
The inset shows the two possible polarizations of the photon, adapted from Refs. [32–34].

cascade. Vanishing FSS of the exciton state is essential to achieve entanglement, which is possible by size tuning (see Figure 2.7 in Refs. [1–3]) but difficult to achieve for QDs grown on (001) substrates. Applying external electrical fields can help to surmount this barrier to achieve FSS = 0 meV. An alternative is to move to a different

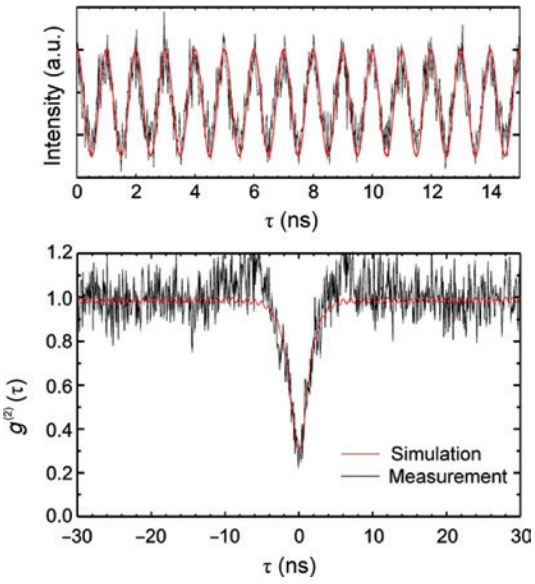

Figure 8: (Top) Optical response of a SPE to an electrical 1-GHz signal with a pulse width of 350 ps and simulation of a pulse train with 400 ps width (red line).
(Bottom) Correlation measurement at the same frequency demonstrates clear antibunching. The red line is a simulation of a pulsed perfect single-photon device ($g^{(2)}(0) = 0$) with 1-GHz repetition rate, taking into account the limited time resolution of 0.7 ns of the setup, from Refs. [32–34].

surface orientation of the substrate, like (111), for the QD growth. Then the rotational symmetry of the QDs is threefold, which is not lowered any more by piezoelectric effects; the excitonic bright states remain degenerate [29, 30]. However, none of the InGaAs QDs SPE emission at room temperature was reported yet. It is straightforward to move to wurtzite structures, like GaN/AlN QDs, which show the advantage of much larger localization energies of the charge carriers and thus larger thermal stability, suggesting room-temperature operation of the SPEs. Recent experiments showed huge fine structure splitting up to 7 meV for GaN/AlN QDs [32–34]. Single photon emission up to RT has been indeed reported for QDs based on the (InGaAl)N material system.

6 Many QDs in semiconductor lasers

In one of the very first ever publications on self-organized QDs, the material gain of InAs QDs was reported to be orders of magnitude larger than that of an identical 3D material and surprisingly larger than theoretically predicted [1–6, 10, 11]. QD dot layers were observed to be easily stacked many times in lasers [10, 11], such that their modal gain is as large as or larger than that of stacked QWs. One of the first important subsequent discoveries was the observation of efficient recombination and lasing at 1.3 μm of InAs QDs inserted in GaAs, a wavelength previously only accessible by InP-based lasers, showing the disadvantage of a large temperature dependence of the threshold current density. Emission wavelengths beyond 1.5 μm were demonstrated for devices grown on metamorphic buffers [1–3]. Important improvements of photonic device properties were based on the introduction of dot-in-a-well structures and p-type doping, leading to temperature independence of the threshold current density up to elevated temperatures of more than 70°C. Consequently, costly and energy-inefficient Peltier coolers for the lasers can be avoided in many systems.

Detailed investigations of QD laser properties showed internal recombination efficiencies close to 100%. Their experimentally observed threshold current densities were found to be as low as 6 A/cm^2 × dot layer, again lower than predicted and at least an order of magnitude lower than for QW lasers. Figure 4B summarizes the development of threshold current densities of semiconductor lasers since their invention.

Twelve-watt output power, equivalent to a power density of 18.2 MW/cm^2, and 100% internal efficiency for a sixfold MOCVD grown stack were reported together with suppressed facet overheating, increasing the catastrophic optical mirror damage (COMD) level. In lifetime tests at 1.0 W and 1.5 W and 50°C heat sink temperature, no aging of these lasers within 3000 h could be observed [1–3]. QD lasers, whatever their application in systems is, present thus the most energy-efficient laser sources known. This is not too surprising, as the excitonic ground state (or any other state) of a QD is saturated and will lase after being filled with only two pairs of electrons and holes. Assuming a realistic dot density of 2.5×10^{10} QDs/cm^2 and a fourfold stack of QD layers, an injection current density of 10^{11} carriers/cm^2 is sufficient to result in saturated lasing of the ensemble of ground states for a lossless device. We are still far from the limit of zero loss. Future work has to focus on reducing them together with the series resistance.

Suppression of filamentation for edge-emitting QD lasers emitting in the 1100–1300-nm range for the transverse ground mode at stripe widths up to 9 μm were observed to lead to superior beam quality (lower M^2) and increased coupling efficiency into fibers, another early discovery [1–3].

At the same time, the sensitivity to optical feedback was analyzed. Quantum well lasers are extremely unstable under optical feedback, forcing often the use of optical isolators in fiber modules or systems. QD lasers emitting on the ground state exhibit a stability enhancement by 23 dB against feedback due to the strong damping of the

relaxation oscillations. A threshold for the coherence collapse of –8 dB has been measured [1–3].

QD lasers are advantageous in large environmental radiation work places like in space. Comparative studies of the influence of high energy proton irradiation on QW and QD lasers show an enhanced radiation hardness of QD lasers. The increase of threshold current density upon irradiation is much less than in QW lasers. In addition, much reduced facet overheating and catastrophic optical mirror damage was demonstrated in this work [1–3].

Gain of the QDs and index of refraction of the light guiding layer are completely decoupled, as the total number of carriers residing in the QDs is many orders of magnitude smaller than the number of carriers residing in the carrier reservoir. From there, the carriers are scattered down to the QDs via Auger effect at a timescale below ps, leading to ultra-fast gain recovery upon gain depletion [35]. Ultrafast gain and phase modulation or both together are independently possible for QD lasers, as will be shown in the next sections.

7 High-frequency directly modulated QD lasers

Fiber to the home systems as the end point of metropolitan (MAN) and access (AN) networks is presently installed in huge quantities in all industrialized countries. MAN traffic hardware installations are forecast to grow significantly faster than long-haul traffic ones. Consequently, the number, diversity, and complexity of high-speed photonic devices, presenting the physical layer of the networks operating at least partly at 1.3 μm, will increase rapidly. Innovative solutions are required to control power consumption and cost of the networks. InAs/GaAs QD-based photonic modules outperform devices based on other material systems or QWs at this wavelength from any point of view, as presented in the previous section. They are more energy efficient, are more temperature stable, and have much lower cost, in particular at the module level, and offer essential properties not observed for higher dimensional devices. The same is true for InAs/InP QD-based photonic modules, which are presently lacking somewhat behind the GaAs-based ones in development.

Directly modulated QD lasers are key components for fiber-based Datacom, MAN, and AN networks. The data rates reported for GaAs QD-lasers based on graded p-type doping emitting at 1.31 μm in the O-band and InP-based QD-lasers emitting at 1.55 μm in the C-band are beyond 25 Gbit/s [36, 37] for large signal direct modulation in the non-return-to-zero (NRZ) on-off keying (OOK) scheme. Emission at QD excited states translates to larger differential gain and smaller nonlinear gain compression as compared to the ground state, being thus advantageous for many applications. In order to increase further the bandwidth of DML lasers, higher order modulation formats such as four- and eight-level pulse-amplitude modulation (PAM) were explored. PAM4 results for O- and C-band lasers demonstrate 17.5-GBd (35-Gbit/s) data transmission for GaAs and InP structures, respectively, (GaAs: graded p-doping). An increase of the maximum bit rate by more than 50% as compared to PAM2 is presently achieved. In PAM schemes (particularly PAM8), the noise level of the lasers becomes the major limiting factor.

A completely different application emerging recently is in automobile industry. Road illumination at night and/or under heavy rain and surround LIDAR systems for general safety and autonomous driving using semiconductor lasers is rapidly diffusing down from high-end cars to mass production. Presently, the lasers used, based on multiple stacked QWs, emit in the 905-nm wavelength range high-power pulses of a typical width of 100 ns. The emission is elliptical, showing e.g. $10^\circ \times 25^\circ$ beam divergence. The optical focusing and scanning systems and temperature stabilization are complex and costly. The maximum laser output power allowed depends on the properties of the human eye and is regulated according to safety classes. For safety class 1, upon moving to emission wavelengths between 1.2 and 1.4 μm, the allowed output power is increased by a factor of ~20. The transmission of air is at a maximum between 1260 and 1340 nm. Thus inexpensive and temperature stable QD lasers available between 1260 and 1310 nm are ideal future sources for road illumination and LIDAR. They can be based on novel HIBBEE high brightness laser structures being astigmatism-free and showing a round far field for as much as 4.2 W cw and 17.7 W pulsed output power at 1060 nm, needing no complex focusing optics [38–40]. The last generation of these lasers is based on QDs. Thus their wavelength can be easily extended to the 1250-nm range. Directly modulated HIBBEE and PBC lasers at 980 and 1060 nm showed pulses down to 70-ps width at modulation rates up to 80 MHz and brightness of 400 MW/cm^{2}sr.

8 Mode-locked QD lasers

"Self-similarity" of QDs does not mean identity. Adjacent QDs do not contain 100% identical number of atoms or identical interfaces but have similar shapes, thus symmetry properties. The emission of, let us say, the active area of a

100-µm wide and 1-mm-long edge emitting laser, containing 10^{11} non-interacting QDs/cm^2, is composed of the emission of 10^8 QDs, each emitting spontaneously at slightly different wavelengths and eventually ordered according to the longitudinal mode selection rules of a laser cavity. Their superposition leads to a Gaussian-shaped envelope of the modes having a half width of 30–100 meV in typical devices, showing finally a hat-like envelope at ground-state saturation. Figure 9 shows such a hat-like structure at 1.3 µm.

The width can be manipulated by growth conditions. The larger the half width on the energy scale, the narrower the pulse width on the time scale, as both are correlated by Fourier transformation. The power of easy generation of fs pulses by mode-locked QD lasers (QD-MLL) in the O- or C-bands, or ultrafast multiple wavelength amplification without cross-talk by QD-based semiconductor optical amplifiers (see next section), results from this Gaussian broadening.

MLLs emitting both electrical and optical pulse trains presently emerge as backbone of high bit-rate optical communication networks both in the O- and C-bands. Generation of shortest optical pulses at frequencies far beyond the intrinsic laser bandwidth is feasible using MLL, where the phases of the longitudinal modes in the laser spectrum are locked [41]. MLLs are utilized as optical clocks, as frequency combs, and, in combination with modulators and wavelength splitters, as transmitters for optical time- and wavelength-division multiplexing (OT/WDM) systems. They also find applications in other fields of communication, such as for multi-carrier generation and all-optical sampling. Still in THz photonics or radio-over-fiber systems, the source/transmitter architecture can be simplified by using MLLs. Passively ML lasers (PMLLs) have the lowest cost, as they only incorporate an additional element in the cavity, a saturable absorber, which,

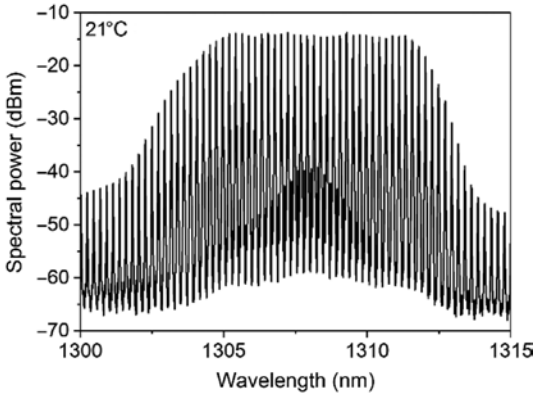

Figure 9: Hat-like distribution of longitudinal modes in a QD-lasers at ground-state saturation compared to low current.

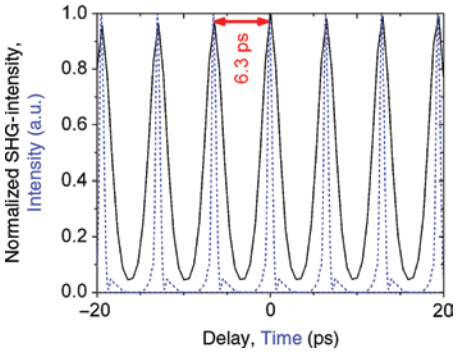

Figure 10: Repetition rate of a chirp compensated QD MLL pulse comb at 160 GHz using an optical time division multiplexer, SHG autocorrelation measurement (black), and corresponding pulse comb (blue).

as well as the gain section, is simply direct current (DC) biased. The absorber ensures self-start of ML, without an external radio-frequency (RF) reference source [42–45].

Saturable absorbers based on QDs emitting at 1.3 µm were shown to exhibit fast recovery on the order of 700 fs under large reverse bias, enabling the generation of low chirp or chirp-compensated, Fourier-limited sub-picosecond pulses at frequencies of or beyond 80 GHZ, taking advantage of the large spectral width of the QD emission [42–45]. The timing jitter of MLLs is a result of random fluctuations of the photon density caused by amplified spontaneous emission (ASE). Compared to QWs, QD MLLs exhibit lower levels of ASE, which directly reduce the jitter. Optical feedback is the method of choice to reduce jitter. Values of 121 fs for the integrated jitter were reported as well as tuning ranges of 300 MHZ around the fundamental mode locking frequency both for QD lasers emitting at 1.31 µm [17, 18] and 1.55 µm [45].

Repetition rates up to 160 GHz[10] are shown in Figure 10.

By means of advanced modulation formats, larger spectral efficiencies, the ability to operate the system at a lower symbol rate for a desired data rate, are feasible and can replace time division multiplexing. Data transmission at 160 Gbit/s based on single-polarization differential quadrature phase shift keying D(Q)PSK data transmission format was demonstrated using a hybrid MLL module combined with modulators [17, 18].

9 QD-based semiconductor optical amplifiers and wavelength switches

In optical networks optical amplifiers, OAs are of the same large importance as transceivers or receivers. Amplifiers

serve as boosters, in-line, or preamplifiers and perform regenerative (2R), wavelength conversion or switching tasks for optical signal processing.

State-of-the-art ANs and MANs use up to 40 wavelength channels, each carrying presently a data stream of typically 10 Gb/s, planned to increase to 40 Gb/s in the very near future. Next-generation optical networks, such as converged MANs and reach extended ANs, will cover longer distances than hitherto and accommodate larger splitting ratios (number of customers). Optical amplifiers are essential to compensate the additional losses caused by the extended reach and larger splitting ratios. Such amplifiers have to support multiple modulation formats, multi-level intensity, and phase-coded formats, as well as multi-wavelength channel amplification with low channel crosstalk. Wavelength switching and switching tasks for optical signal processing e.g. by cross-gain-modulation at ultimate bit rates comprise additional challenges. Low energy consumption and low cost will be equally decisive parameters in the future as maximum bit rate, to keep not only investment down but also end of life cost and environmental damages.

Semiconductor OAs are low-cost mass products, showing reduced power consumption, smaller footprint, ease of integration in photonic integrated circuits, and broader gain spectra as compared to other types of amplifiers. At wavelengths around 1310 nm, QD SOAs are the only available amplifiers performing at the same time all tasks necessary as mentioned above [19]. QD-based amplifiers offer large advantages as compared to classical ones: broad but fixed bandwidth due to QD size distribution, ultra-fast gain recovery of ~100 fs [35] for high-speed amplification, reduced chirp due to a low alpha factor [46, 47] enabling fast switching, and intrinsically strongly damped relaxation oscillations [47] yielding low patterning effects. Decoupling of gain and phase dynamics enables to operate QD-SOAs easily under phase modulation or at higher order modulation formats like DQPSK [19]. Operation including higher excited states enables additional enormous broadening of the bandwidth [36, 37].

The fast gain dynamics of QD SOAs has been demonstrated to enable single channel amplification of ultra-short pulses with sub-picosecond width. A QD ML laser operating at 42.7 Gbit/s presented in the previous section was fiber-coupled to a SOA of the same QD gain material. Pulses at 710 fs in the pulse train were amplified by a 4-mm-long QD SOA. The maximum chip gain of this device was 26 dB. No increase of the bit error rate up to 45 km by the QD SOA could be observed for 42.7-Gbit/s NRZ OOK signals, as demonstrated in Figure 11.

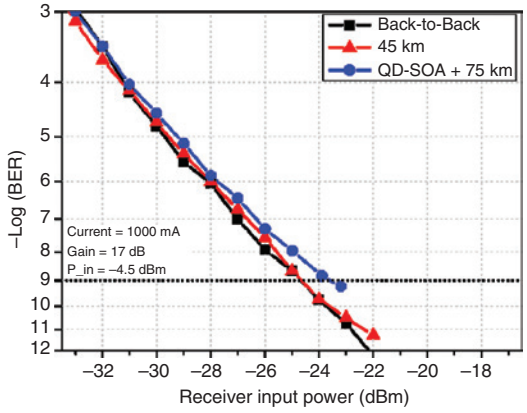

Figure 11: Bit error rates of a 42.7-Gbit/s NRZ OOK signal from a QD MLL and a QD SOA across 45 and 75 km compared to a back-to-back BER measurement of the QD MLL.
Up to 45 km, no power penalty is found. The power penalty at 75 km is as low as 1 dB, adapted from Refs. [19] and [41].

Multi-channel amplification of intensity-coded signals with symbol rates up to 320 Gbit/s was recently shown. Thus QD-SOAs can operate at the same time in downstream as well as upstream modes, reducing cost and power consumption by 50%.

Fast processing of optical data, such as switching and wavelength conversion, presents the key for the implementation of all-optical AN and MAN networks. Signal processing in the optical rather than in the electrical domain offers numerous advantages like avoiding multiple optical-electrical conversions, enabling simpler systems, and having enhanced bandwidth and transparency to modulation formats [19]. The most important requirements for nonlinear components performing these tasks are low cost, low power consumption, and small footprint.

Three different nonlinear effects in semiconductor gain materials are commonly employed for wavelength conversion: cross-gain modulation (XGM), cross-phase modulation (XPM), and four-wave mixing (FWM), see Figure 12.

FWM-based conversion offers a very large bandwidth; high extinction ratio, amplitude, and phase sensitivity; inversion of the spectral phase; as well as a large conversion range, if a multiple-pump configuration is used. The conversion efficiency and optical signal-to-noise ratio (OSNR) were improved to positive conversion efficiencies and OSNRs larger than 25 dB. FWM in QD SOAs has been demonstrated for various modulation formats and data rates up to 320 Gbit/s [19].

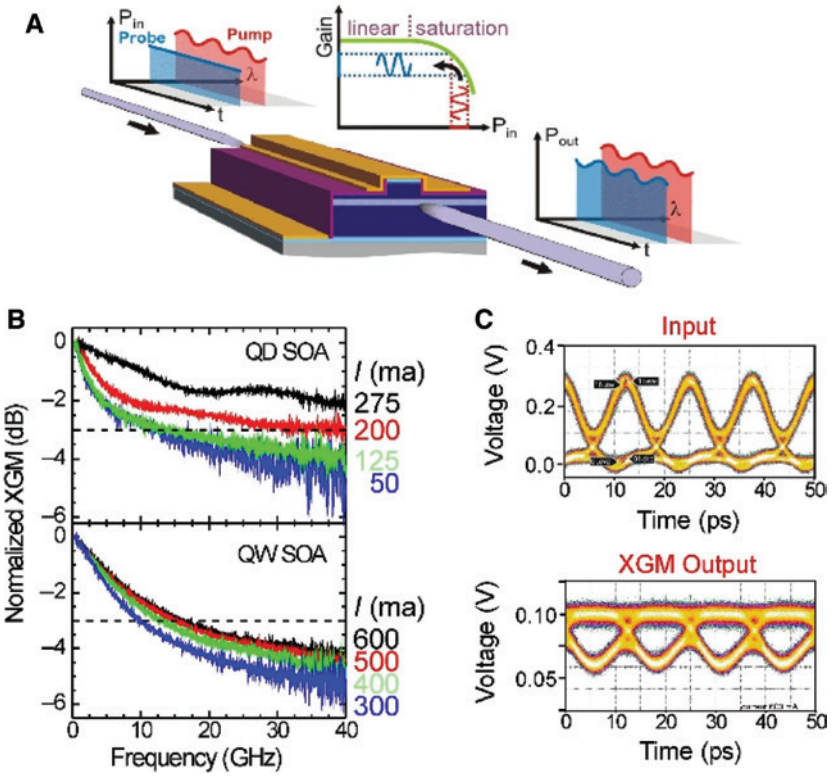

Figure 12: Cross-gain modulation of a semiconductor optical amplifier (SOA).
The figure shows schematically a ridge waveguide structure, having a ridge width 2–4 μm, beginning with the substrate, the waveguide, and "the dots in a well" amplifying layers (from bottom to top). (A) Operation principle: a strong, modulated pump signal (P_{in}, red) drives the SOA in the saturation regime. Consequently, the SOA gain is also modulated. The modulation pattern can be transferred to a weak CW probe pulse at another wavelength (P_{in}, blue), yielding a modulation pattern inverted to the probe signal at the output (P_{out}, blue). (B) Efficiency of the cross-gain modulation of a QD SOA (top) and a conventional QW SOA (bottom). The 3-dB bandwidth of the QD SOA marked by the horizontal line can be tuned to beyond 40 GHz at high injection current. (C) Wavelength up-conversion using cross-gain modulation of a QD SOA for a pseudorandom RZ-OOK modulation. Top: input eye diagram of 80-Gb/s signal at 1292-nm wavelength, bottom: upconverted output signal at 1300 nm, from Ref. [4].

10 Conclusions

The growth of semiconductor QDs is based on strain-driven self-organization effects, being universal for any non-lattice-matched heterostructure. The electronic and optical properties of QDs are simpler than those of the simplest atom, hydrogen. All energy levels are only twofold degenerate. The density of states of the electron and hole levels are described by a delta-function showing in emission a finite coherence time-controlled Lorentzian broadening. The emission from single dots is governed by excitonic effects, induced by the strong Coulomb interaction of the charges closely localized in space. This emission is polarized, and size-dependent fine structure splitting is observed.

Single localized QDs inserted in LEDs show emission of quantum bits of perfect fidelity at frequencies up to 1 GHz. QDs grown on (111) GaAs substrates or in general wurtzite type substrates, showing a threefold crystal symmetry, are potential sources of entangled photons.

Emission from ensembles of many QDs shows Gaussian broadening. The emission of InAs/GaAs QDs, which was presented in detail, can be tuned beyond 1.3 μm, thus covering a wavelength range normally not accessible for GaAs-based devices. Lasers and amplifiers with multiple stacks of QDs as gain areas show continuous and dynamic properties much superior to those of quantum well based devices of the same material system. Frequency combs up to 160 GHz and pulses of widths and timing jitter below 1 ps are generated by mode-locking at 1.3 μm. Amplification by QD-SOAs of 26-dB chip gain of 710-fs pulses without any broadening as well as multi-channel amplification of intensity-coded signals with bit rates up to 320 Gbit/s is reported. Four wave mixing for wavelength conversion is

demonstrated for various modulation formats and data rates up to 320 Gbit/s.

Based on both the insights on optimum growth of QDs, partly presented here, and of growth of III–V materials on Si, in the last few years, enormous progress has been made on integration of active photonic devices on Si [48, 49]. This research could not be presented here, meriting its own review.

Acknowledgments: It is with great pleasure to thank my former and present co-workers, as well as colleagues and friends all around the world, who decisively contributed to the results reported here. Among them are as follows: Dejan Arsenijevic, Paola Borri, Jürgen Christen, Gerrit Fiol, Marius Grundmann, Frank Heinrichsdorff, Axel Hoffmann, Nils Kirstaedter, Matthias Kuntz, Matthias Lämmlin, Nicolai Ledentsov, Anatol Lochmann, Christian Meuer, Udo Pohl, David Quant, Sven Rodt, Andrei Schliwa, Holger Schmeckebier, Robert Seguin, Vitali Shchukin, Oliver Stier, Erik Stock, André Strittmatter, Mirko Stubenrauch, Volker Türck, Waldemar Unrau, Victor Ustinov, Till Warming, and many others, who hopefully forgive me for not mentioning them although they would have deserved it.

References

[1] Bimberg D. Semiconductor quantum dots: Genesis – the excitonic zoo – novel devices for future applications. In: Kaminov IP, Li T, Willner AE, eds. Optical fiber telecommunications V A. Amsterdam, Elsevier, 2008, 23–52.
[2] Sellin RL, Ribbat C, Bimberg D, et al. High-reliability MOCVD-grown quantum dot laser. Electr Lett 2002;38:883–4.
[3] Huyet G, O'Brien D, Hegarty S, et al. Quantum dot semiconductor lasers with optical feedback. Phys Stat Sol (a) 2004;201:345–52.
[4] Bimberg D, Pohl UW. Quantum dots: promises and accomplishments for novel devices. Mater Today 2011;14:388–98.
[5] Klimov VI. Spectral and dynamical properties of multiexcitons in semiconductor nanocrystals. Ann Rev Phys Chem 2007;58:635–73.
[6] Bimberg D, Grundmann M, Ledentsov NN. Quantum dot heterostructures. Chichester, John Wiley & Sons, 1998.
[7] Shchukin VA, Bimberg D. Strain driven self-organization of nanostructures on semiconductor surfaces. Appl Phys A 1998;67:687–700.
[8] Haken H. Synergetics, an introduction: nonequilibrium phase transitions and self-organization in physics, chemistry and biology. Berlin, Springer, 1983.
[9] Ruvimov S, Werner P, Scheerschmidt K, et al. Structural characterisation of (InGa)As quantum dots in a GaAs matrix. Phys Bev B15 1995;51:14766–9.
[10] Heinrichsdorff F, Krost A, Grundmann M, et al. Self-organization processes of InGaAs/GaAs quantum dots grown by metalorganic chemical vapor deposition. Appl Phys Lett 1996;68:3284–6.
[11] Schmidt OG, Kirstaedter N, Ledentsov NN, et al. Prevention of gain saturation by multi-layer quantum dot lasers. Electr Lett 1996;32:1302–4.
[12] Meixner M, Schoell E, Shchukin VA, Bimberg D. Self-assembled quantum dots: crossover from kinetically controlled to thermodynamically limited growth. Phys Rev Lett 2001;87:236101.
[13] Michler P, Kiraz A, Becher C, et al. A quantum dot single-photon turnstile device. Science 2000;290:2282–5.
[14] Kloeffel C, Loss D. Prospects for spin-based quantum computing in quantum dots. Ann Rev Condensed Matter Phys 2013;4:51–81.
[15] Unrau W, Bimberg D. Flying qubits and entangled photons. Lasers Photonics Rev 2014;8:276–90.
[16] Geller M, Marent A, Bimberg D. Nanomemories using self-organized quantum dots. In: Sattler KD, ed. Handbook of semiconductors 6: nanoelectronics and nanophotonics. Boca Raton, CRC Press, 2011, 2-1–26.
[17] Arsenijevic D, Bimberg D. Quantum-dot mode-locked lasers: sources for tunable optical and electrical pulse combs. In: Eisenstein G, Bimberg D, eds. Green photonics and electronics. Heidelberg, Springer, 2017, 75–106.
[18] Schmeckebier H, Fiol G, Meuer C, Arsenijevic D, Bimberg D. Complete pulse characterization of quantum-dot mode-locked lasers suitable for optical communication up to 160 Gbit/s. Optics Expr 2010;18:3415–25.
[19] Schmeckebier H, Bimberg D. Quantum-dot demiconductor optical amplifiers for energy-efficient optical communication. In: Eisenstein G, Bimberg D, eds. Green photonics and electronics. Heidelberg, Springer 2017, 37–74.
[20] Dingle R, Henry C. Quantum effects in heterostructure lasers, United States Patent Office 1976, 3 982 207.
[21] Asada M, Miyamoto Y, Suematsu Y. Gain and threshold of three-dimensional quantum box lasers. IEEE J Quantum Electron 1986;22:1915–21.
[22] Arakawa Y, Sakaki H. Multidimensional quantum well lasers and temperature dependence of its threshold current. Appl Phys Lett 1982;40:939–41.
[23] Hirayama H, Matsunaga K, Asada M, Suematsu Y. Lasing action of $Ga_{0.67}In_{0.33}As$/GaInAsP/InP tensile-strained quantum box lasers. Electron Lett 1994;30:142–3.
[24] Grundmann M, Christen J, Ledentsov NN, et al. Ultranarrow luminescence lines from single quantum dots. Phys Rev Lett 1995;74:4043–6.
[25] Kirstaedter N, Ledentsov NN, Grundmann M, et al. Low threshold, large T_o injection laser emission from (InGa)As quantum dots. Electr Lett 1994;30:1416–7.
[26] Lenz A, Timm R, Eisele H, et al. Reversed trunacted cone distribution of $In_{0.8}Ga_{0.2}As$ quantum dots overgrown by an $In_{0.1}Ga_{0.9}As$ layer in a GaAs matrix. Appl Phys Lett 2002;81:5150–2.
[27] Stier O, Grundmann M, Bimberg D. Electronic and optical properties of strained quantum dots modeled by 8 band-band k.p theory. Phys Rev 1999;59:5688–701.
[28] Ustinov VM, Zhukov AE, Egorov AY, et al. Low threshold quantum dot injection laser emitting at 1.9 μm. Electr Lett 1998;34:670–2.
[29] Walther T, Cullis AG, Norris DJ, Hopkinson M. Nature of Stranski-Krastanow transition during epitaxy of InGaAs on GaAs. Phys Rev Lett 2001;86:2381–3.

[30] Schliwa A, Winkelnkemper M, Bimberg D. Few-particle energies versus geometry and composition of $In_xGa_{1-x}As$/GaAs self-organized quantum dots. Phys Rev B 2009;79:075443.
[31] Schliwa A, Hoenig G, Bimberg D. Electronic properties of III–V quantum dots. In: Ehrhardt M, Koprucki T, eds. Multi-band effective mass approximations. Berlin, Springer, 2014, 57–85.
[32] Bimberg D, Stock E, Lochmann A, et al. Quantum dots for single-and entangled-photon emitters. IEEE Photonics J 2009;1:58–68.
[33] Kindel C, Kako S, Kawano T, et al. Exciton fine-structure splitting in GaN/AlN quantum dots. Phys Rev B 2010;81:241309.
[34] Holmes MJ, Choi K, Kako S, Arita M, Arakawa Y. Room-temperature triggered single photon emission from a iii-nitride site-controlled nanowire quantum dot. Nano Lett 2014;14:982–6.
[35] Borri P, Schneider S, Langbein W, Bimberg D. Ultrafast carrier dynamics in InGaAs quatum dot materials and devices. J Opt A Pure Appl Opt 2006;8:S33–48.
[36] Arsenijević D, Bimberg D. Quantum-dot lasers for 35 Gbit/s pulse-amplitude modulation and 160 Gbit/s differential quadrature phase-shift keying. Proc SPIE 2016;9892:98920S1–9.
[37] Gready D, Eisenstein G, Ivanov V, et al. High speed 1.55 μm InAs/InGaAlAs/InP quantum dot lasers. IEEE Phot Technol Lett 2014;26:11–3.
[38] Miah Md J, Kalosha VP, Bimberg D, Pohl J, Weyers M. Astigmatism-free high-brightness 1060 nm edge-emitting lasers with narrow circular beam profile. Optics Express 2016;26:30514–22.
[39] Posilovic K, Kalosha VP, Winterfeldt M, et al. High-power low-divergence 1060 nm photonic crystal laser diodes based on quantum dots. Electr Lett 2012;48:1419–20.
[40] Riecke S, Posilovic K, Kettler T, et al. 10.7 W peak power picosecond pulses from high-brightness photonic crystal laser diode. Electr Lett 2010;46:1393–4.
[41] Schell M, Weber AG, Schoell E, Bimberg D. Fundamental limits of sub-ps pulse generation by active mode-locking of semiconductor lasers: the spectral gain width and the fact reflectivities. IEEE J Quant Electr 1991;27:1661–8.
[42] Kuntz M, Fiol G, Laemmlin M, et al. Transform-limited optical pulses from 18 GHz monolithic mode-locked QD lasers operating at 1.3 μm. Electr Lett 2004;40:346–7.
[43] Rafailov EU, Cataluna MA, Sibbett W. Mode-locked quantum-dot lasers. Nature Photonics 2007;1:395–401.
[44] Thomson MG, Rae AR, Xia M, Penty RV, White IH. InGaAs quantum-dot mode-locked laser diodes. IEEE J Select Topics Quantum Electr 2009;15:661–72.
[45] Sadeev T, Arsenijević D, Franke D, Kreissl J, Künzel H, Bimberg D. 1.55 μm mode-locked quantum-dot lasers with 300 MHz frequency tuning range. Appl Phys Lett 2015;106:31114-1–4.
[46] Martinez A, Lemaitre A, Merghem K, Ferlazzo L, Dupuis C, Ramdane A. Static and dynamic measurements of the alpha-factor of five-quantum-dot-layer single-mode lasers emitting at 1.3 μm on GaAs. Appl Phys Lett 2005;86:211115–7.
[47] Kuntz M, Ledentsov NN, Bimberg D, et al. Spectrotemporal response of 1.3 μm quantum-dot lasers. Appl Phys Lett 2002;81:3846–8.
[48] Mi Z, Yang Y, Bhattacharya P, et al. High-performance quantum dot lasers and integrated optoelectronics on Si. Proc IEEE 2009;97:1239–49.
[49] Wan YT, Zhang ZY, Chao RL, et al. Monolithically integrated InAs/InGaAs quantum dot photodetectors on Si substrates. Opt Express 2017;25:27715–23.